On the fit of skins with a particular focus on the biomechanics of loose skins of hagfishes[1]

T.A. Uyeno and A.J. Clark

Abstract: There is a considerable diversity in how skins fit. Here, we review the function of both tight and loose skins and note that the latter are poorly understood. Analysis of loose skin examples suggest five functional categories: (I) freedom of movement, (II) surface area enhancement, (III) increased structural extensibility, (IV) lubrication, and (V) maladaptive examples arising through sexual or artificial selection. We investigate the skins of hagfishes as a model for understanding loose skin function by examining its structure using histology, standardized puncture resistance testing using the ASTM F1306 protocol, and the effect of internal pressure using a simple inflated balloon model. Skins of hagfishes are composed of multiple layers of cross-helically wound connective tissue fibers of a 45° angle to the longitudinal axis, resulting in a skin that functions as fabric cut "on the bias". Hagfish skins are relatively yielding; however, skin looseness adds a "structural extensibility" that may allow hagfishes to compensate for low puncture resistance. Physical balloon models, with stiff cores that limit length changes, show that only low pressures allow short loop radii without local buckling. Hagfishes represent ideal organisms for studying loose skin function because their skins seem to fit in all functionally adaptive categories.

Key words: puncture resistance, loose skin, physical model, *Myxine glutinosa*, Atlantic hagfish, *Eptatretus stoutii*, Pacific hagfish.

Résumé : L'ajustement de la peau sur le corps présente une grande diversité. Nous présentons une synthèse de la fonction des peaux tendues et lâches et notons que les peaux lâches sont mal comprises. L'analyse d'exemples de peau lâche fait ressortir cinq catégories de fonctions, à savoir : (I) liberté de mouvement, (II) accroissement de la superficie, (III) extensibilité structurale accrue, (IV) lubrification et (V) exemples mal adaptés découlant de la sélection sexuelle ou artificielle. Nous étudions les peaux de myxine comme modèle pour comprendre la fonction des peaux lâches et, pour examiner leur structure, avons recours à l'histologie, des essais normalisés de résistance au percement basés sur le protocole F1305 de l'ASTM et l'effet de la pression interne à l'aide un modèle simple de ballon gonflé. Les peaux de myxine sont composées de multiples couches de fibres de tissu conjonctif entrecroisées selon un motif hélicoïdal à 45° par rapport à l'axe longitudinal, produisant ainsi une peau qui se comporte comme un tissu coupé « sur le biais ». Si les peaux de myxine sont assez souples, leur caractère lâche leur confère une plus grande « extensibilité structurale » qui pourrait faire contrepoids à leur faible résistance au percement. Des modèles physiques de ballon, dotés de noyaux rigides qui limitent les variations de longueur, montrent que seules de faibles pressions permettent de courts rayons de boucle sans vrillage local. Les myxines sont des organismes tout désignés pour l'étude de la fonction des peaux lâches, puisque leur peau semble s'inscrire dans toutes les catégories d'adaptations fonctionnelles. [Traduit par la Rédaction]

Mots-clés : résistance au percement, peau lâche, modèle physique, *Myxine glutinosa*, myxine du nord, *Eptatretus stoutii*, myxine du Pacifique.

Introduction

Background

> When a man's condition does not suit him, it will be as a shoe at any time; which, if too big for his foot, will throw him down; if too little, will pinch him. — Horace

Rather than human fortunes, the Roman poet Horace (Smart 1885) could have been comparing organismal integuments to ill-fitting shoes. Presumably, evolution confers upon animals a skin that fits just right; one that is voluminous enough to contain the requisite "guts and gonads" (Daley and Usherwood 2010), yet not too loose as to incur exorbitant construction and maintenance costs or to impede physical interactions with the surrounding physical world. However, one does find a diversity of skin sizes that range from being tightly stretched over a body core to being floppy and loose fitting. This raises the functional question of why? What are the adaptive benefits of skin that appears to be ill fitting? A brief survey of the literature suggests a plethora of studies that focus on tight integuments, but fewer investigate the other end of the spectrum. Thus, in this study, we review the adaptive benefits of taut skins and then focus on skins that fit loosely. Although we review loose skins of many organisms, we are reminded of Krogh's (1929) principle, in which, for any given

T.A. Uyeno. Department of Biology, Valdosta State University, 1500 North Patterson Street, Valdosta, GA 31698, USA.
**A.J. Clark.** Department of Biology, College of Charleston, 66 George Street, Charleston, SC 29424, USA.
Corresponding author: T.A. Uyeno (email: tauyeno@valdosta.edu).

Fig. 1. Body shape, sheath-core morphology, and looseness index models for two species of fishes: (A) the crescent gunnel (*Pholis laeta* (Cope, 1873)), a taut-skinned elongate teleost, and (B) the Pacific hagfish (*Eptatretus stoutii*), a loose-skinned elongate agnathan. Beneath each species is a digital photograph of a transverse section through the body positioned above a three-dimensional cartoon depicting the section's sheath, or skin, and body core at approximately 50% total length accompanied by a simple geometric model that illustrates the looseness index in the species. Color version online.
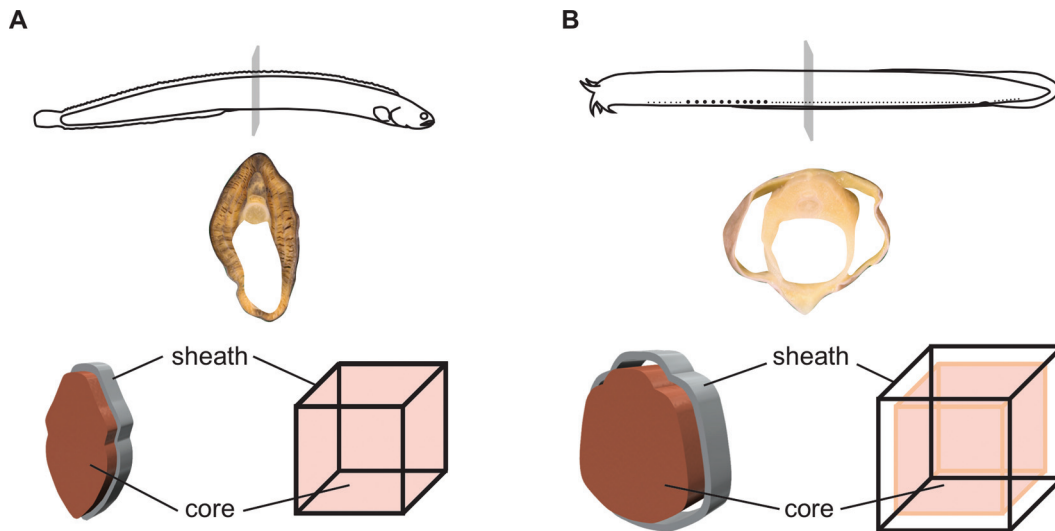
problem, there will be an animal of choice on which the phenomenon can be most conveniently studied. We believe hagfishes to be the best model in which to initially study the functionality of loose skins.

Skin may be one of the most fundamental anatomical features possessed by an organism because it represents the division between the outside world and the controllable environment within. Mirroring organismal size diversity, skin thicknesses have a great range; from the 5–10 nm thick cell membranes that are formed of phospholipid bilayers and embedded proteins of prokaryotes (El-Hag and Jayaram 2008) through eight orders of magnitude to the thick 30.5 cm skin of the bowhead whale (*Balaena mysticetus* Linnaeus, 1758) that contains an insulating layer of blubber (Rugh and Shelden 2009). If one considers other functions of skin, then we find a considerable diversity of uses beyond forming a boundary. In arthropods, chitinous skins serve as rigid external skeletal structures and as tough armor (Vincent and Wegst 2004; Clark and Triblehorn 2014). Many animals protect their soft tissues by reinforcing their skins; sea stars and sea cucumbers, sharks, and armadillos incorporate rigid dermal elements (e.g., Stricker 1985; Yang et al. 2012). Skin may also provide more than simple mechanical armor. Integuments may also include adaptions that block damaging radiation, such as our own epidermal production of melanin in the presence of ultraviolet radiation (Brenner and Hearing 2008). In aquatic environments, osmoregulators better manage the osmotic flux if they possess relatively impermeable integuments, as is found in scaly fish skins (Potts et al. 1967). Skins may also be otherwise impermeable; they may provide insulation to help maintain internal temperatures within a physiologically optimal range (e.g., in mammals; Ryg et al. 1993). Rather than a barrier, skins may be used as a method of uptake. If the skin is capable of cellular uptake of valuable resources such as water, oxygen, and dissolved organic matter, then the body's skin represents a surface area to be used in feeding and respiration. Examples include toad skins, through which water may be absorbed (Viborg and Hillyard 2005), and the absorptive tegument of tapeworms and flukes that allows direct uptake of nutrients from the host digestive system (Dalton et al. 2004). Finally, an animal's skin often provides control over

body geometry. This seems obvious in animals with hard exoskeletons, but it also occurs in soft-bodied animals. Here, the flexible tensile wrappings within the skin may allow animals such as nematodes to contain high hydrostatic pressure and limit body deformations (Clark and Cowey 1958). Regardless of the nature of the structural support system, the skin represents the interface between the organism and its physical world (Vogel 2013). Thus, being "where the rubber meets the road", skins, and their characteristics, influence how animals may interact with the air, water, or ground that surround it.

To investigate the adaptive benefits of various skin fittings, we found it useful to define a conceptual "looseness index". Here, we model an organismal body as a simple skin (the sheath) that surrounds its contents (the core) (Figs. 1A and 1B). The sheath may enclose a relatively smaller, equal, or be stretched to fit a relatively larger core volume. Indeed, throughout development or, as some sheaths may be active due to the inclusion of muscle tissue, this relationship may even vary over long and short terms. Consider the sheath and core volumes separately; if one removes a tight sheath that is stretched around its core, then its unloaded volume of the sheath will be less than the volume of the core. When defining the looseness index, a ratio of sheath volume divided by core volume, this tight sheath would have an index value of less than one. Conversely, a loose sheath that contains a core with extra volume to spare would constitute a looseness index of greater than one. Finally, a sheath without any tension or slack, that exactly surrounds the volume of its core, defines a looseness index of one.

Tight skins

Tight skins, both natural and manmade, with a looseness index below unity, have been the subject of many studies. A brief review of tight skins highlights common anatomical features as illustrated by three examples.

Skins that are stretched or pressurized are often reinforced with tensile fibers that are wound around the body (Wainwright et al. 1978). These fibers tend to be present in two opposing orientations to resist pressure in a symmetrical fashion. Tensile fibers that are tightly wrapped around a cylindrical core may be arranged in two contrasting orientations; fibers may run lengthwise (parallel

to, or 0° from, the longitudinal axis) and circumferentially (hoopwise, or 90° from, the longitudinal axis) or may be offset in right- and left-hand helices (at an angle in between 0° and 90°) (Vogel 2013). Although both fiber orientations resist pressure, they differ in how they respond to deformation. Lengthwise and hoop-oriented fibers best resist forces that pull or push along the long axis of the cylinder and confer upon it a relatively high flexural stiffness (Koehl et al. 2000). Helically wound fibers resist twisting forces and will bend readily with less kinking (local buckling) relative to cylinders with lengthwise and hoop-oriented fibers (Vogel 2013).

Nematodes, or roundworms, represent one of the most successful phyla on earth. They are interesting here because their taut sheathes withstand high internal pressures. Harris and Crofton (1957) first measured this unusually high pressure and noted that it was contained by helically wound fibers of a very specific angle of 54.7°. Clark and Cowey (1958), who had earlier discovered a similar helical fiber angle in high-pressure nemerteans (ribbon worms), gave an excellent geometrical explanation for this angle: it is the helical winding angle that, when wrapped around a flexible cylinder of constant volume, allows for the maximum core volume and a looseness index of exactly one. If the cylinder's volume is less than maximal, then any deformations would allow for changes in length (as the tensile fiber angles decreases and become more lengthwise) or in girth (as the fiber angles increase and become more hoop-like). In these worms, body deformations that could cause body volume changes immediately place the helical skin fibers in tension and increase internal pressure or turgor (and reduce the looseness index). Such hydrostatic pressure is used by roundworms, which lack circular muscles, as stiff skeletal support against which longitudinal muscles may act antagonistically (Kier 2012).

Fast moving fish, such as sharks, also use tight fitting skins with crossed-helical fiber arrays that resist deformations. Wainwright et al. (1978) noted that this allowed the body to stiffen hydrostatically. This hydrostatic skeleton, more so than the cartilaginous endoskeleton, transmits muscular locomotory contractions to the sheath. These authors used the word "exotendon" to describe the skin of sharks because it directly transferred the force generated by the muscle to the locomotory surfaces of the skin. This particular function of the skin has also been described in American eels (*Anguilla rostrata* (LeSueur, 1817)) (Hebrank 1980) and several other species of sharks (Naresh et al. 1997). However, additional studies have shown that many species of fishes do not use their skins like exotendons (Hebrank and Hebrank 1986; Summers and Long 2005; Clark et al. 2016) and that the methods for generating thrust can vary between species (Long et al. 1996, 2002*a*; Müller and Van Leeuwen 2006; Kenaley et al. 2018). Nonetheless, taut body coverings are effective in limiting the amount of whole-body deformation achieved during swimming, and therefore, minimize drag.

Human engineering designs also make use of tight fitting or compression skins. Since 2010, with the banishment of buoyant and hydrophobic polyurethane racing swimsuits (Falcone et al. 2010), Olympic swimmers have reverted to swimsuits that minimize drag by smoothing the surface and reducing deformation through compression (Trinidad Morales et al. 2019). Another example is the Swiss "Libelle" anti-gravity suit that allows fighter jet pilots to withstand up to nine times the force of gravity during rapid turns. The United States Air Force assessment of this suit (Hoepfner et al. 2004) noted that it compresses areas in which blood tends to pool by incorporating hydrostatic sacks of fluid. This style of suit diverges from commonplace pneumatic flight suits and, interestingly, reverts to concepts developed by the original inventor, Dr. Wilbur Franks, who tested his design by noting that mice survived centrifuge rides if their bodies were inserted into water-filled condoms (Hoepfner et al. 2004).

Loose skins

Fewer studies have considered the adaptive benefits of skins with a looseness index that is greater than one. Oversized skin is often baggy because of a loose mechanical connection between the sheath and the core. Often the space between the outer surface of the core and the inner surface of the sheath is filled with fluid or low-density tissue. Oversized skin can also be thrown into folds and appear wrinkly because the subdermal space may be reduced, while maintaining the surface area of the oversized sheath. Octopuses seem to be able to vary the looseness index of their dynamic skins continuously (Allen et al. 2014). Regardless, any reinforcing fibers in the sheath are not normally under tension as they are in taut skins. The analysis of our literature survey (summarized in Table 1) allowed us to establish five, non-mutually exclusive, functional categories of loose skins:

I. Freedom of movement — a loose sheath allows for a greater range of core motion than does a tight sheath of similar compliance. This is especially true in cases where the sheath is itself limited in its motion by its surrounding environment. Such is the case in hearts that must beat within their pericardia and in burrowing rodents, like naked mole-rats (*Heterocephalus glaber* Rüppell, 1842), that must turn around in burrows which are narrow enough to be in contact with the animal's skin. Loose skins themselves also have the freedom to pucker around incisions for closure and healing (Kennedy and Cliff 1979). In our survey, freedom of movement seemed to be the most common reason for loose skins.

II. Enhanced surface area — a sheath with a high looseness index may benefit from an increased surface area over which to absorb, diffuse, or radiate. Of course, having a relatively higher surface area for a given body volume may also be a disadvantage in a different environment. For instance, although oxygen uptake may be improved with added surface area, if that same surface area is used in aquatic locomotion, then it may represent a flappy structure with a high drag coefficient (Vogel 2013).

III. Increased structural extensibility — in order for a rigid structure (such as a pointy tooth) to be able to puncture a sheath, the tooth must be applied with enough force to pierce the material. This force is applied immediately on contact in taut sheaths; however, the loose sheath must be deformed and stretched until it can begin to take on tension. This "pre-de-stressed" nature of loose sheaths may allow for a greater extensibility (and perhaps some important "wiggle room" for the delicate core) despite a potentially reduced peak strength (resulting from a greater curvature of the sheath fibers once they are exposed to tension).

IV. Lubrication and biotribology — reduction of friction and wear is important in human engineering and also in biology. Where humans may use greases and oils to lubricate nested tubing in a telescoping antenna, animals may solve the problems by adding layers of loose skin to reduce friction of one rigid element sliding relative to another.

V. Disadvantageous examples — although there may be functionalities that we have not considered, the examples that did not fit into the previous four categories tended not to be advantageous. Many of the examples here have evolved through sexual or artificial selective pressures.

Loose skin model

None of the categories of loose skin function are mutually exclusive. For example, if a lion's (*Panthera leo* (Linnaeus, 1758)) belly skin is loose because it allows for an increased extensibility

Table 1. A list of examples of loose skins found in nature and human engineering.

Example	I. Freedom of movement	II. Enhanced surface area	III. Increased extensibility	IV. Biotribology	V. Non-advantageous
Biological examples					
Skins of hagfishes	Knotting and knot manipulation (Haney et al. 2020)	Uptake of dissolved organics (Glover et al. 2011)	Surviving shark bites (Uyeno and Clark 2016; Boggett et al. 2017)	Knot sliding (Haney et al. 2020)	
Skins of moray eels	Knotting, moving in crevices (Barley et al. 2016; Caudle et al. 2019)				
Octopus and cuttlefish skin			Texture control, communication (Allen et al. 2014)		
Blob sculpin (*Psychrolutes phrictus* Stein and Bond, 1978)					Not actually loose at depth. Encapsulates gelatinous tissue (Gerringer et al. 2017)
Belly skin of lions (*Panthera leo*)	Expansion for food intake (Turner 1997; Thapar 2004)		Protection against hoof kicks (possibly apocryphal)		
Sharpei dog wrinkles					Selective breeding — harbors parasites and moisture (Muller 1990)
Human pericardial membrane				Reduces friction of beating heart (Moghani et al. 2007)	
Human elbow and knee skin	No binding over range of motion (Verberkt et al. 2013)				
Naked mole-rat (*Heterocephalus glaber*)	When burrowing can turn in skin (Griffin 2008)		Cut skin can seal by contraction (Davidson 1998)		
Grazing animals with extensive panniculus muscle	Shake biting flies off coat (Naldaiz-Gastesi et al. 2018)				
Terrestrial frogs	Accommodates extension of frog leg during jumping?				
Aquatic frogs and hellbenders		Cutaneous respiration (Voute 1963; Guimond and Hutchison 1973)	Puncture resistance?		Correlated skin looseness to male frog mating call pitch (Zheng 2019)
Dewlaps and wattles (e.g., turkeys, elands, anoles)					Sexual selection or signaling (Driessens et al. 2015) — often gets damaged in fights
Indian rhinoceros (*Rhinoceros unicornis* Linnaeus, 1758)	Allows for movement under a hard but loose suit of armor (Shadwick et al. 1992)				
Mammalian scrotums		Control testes temperature (Moore and Quick 1924)			

Table 1 (*concluded*).

Example	I. Freedom of movement	II. Enhanced surface area	III. Increased extensibility	IV. Biotribology	V. Non-advantageous
Mammalian foreskins	Allows for dramatic change in volume (Collier 2011)			Reduces friction during sex (Collier 2011)	
Dog scruffs	Allows for water to be shed centripetally (Dickerson et al. 2012)	Convenient handle for mother?			
Elephant wrinkles		Trap moisture to enhance cooling (Lillywhite and Stein 1987)			
Hedgehog skin	Raising and lowering spines (Bexton 2016)				
Chameleon projectile tongues				Layered skin folds provide lubrication during extension (de Groot and van Leeuwen 2004)	
Kalyptorhynch flatworm hook-bearing proboscides				Reduces friction during hydraulic proboscis extension (Smith et al. 2015)	
Cerata of aeolid nudibranchs		Increased digestive and respiratory surface area (Miller and Byrne 2000)			
Skins of snakes	Pre-stretched prior to molting (Lillywhite 1989)				
Human engineering examples					
Loose-sheath optical fiber cables (gel-filled loose tubes)	Increased tensile strength and resistance to bending breakage (Nothofer and Lausch 2009)				
Mesh diving suits (i.e., shark resistant)	Prevents armor binding (Sullivan 1982)				
Climbing rope with a sheath and core (kernmantle) design	Sheath looseness regulates rope stiffness (Hess 2008)				
Concrete slab slip sheets	Allows for shifting between ground and foundation slab (ACI 2006)				
CV joint boot	Deforms during steering (Grabaum et al. 2000)				

before tearing when it catches a hind hoof of a fleeing zebra (*Equus quagga* Boddaert, 1785), that same loose skin may improve heat dissipation, allow for unfettered movement during full-speed running, or permit additional distention of the abdomen to accommodate large meals (Turner 1997; Thapar 2004). As such, it becomes difficult to tease apart primary and accessory functions of skin looseness. To begin investigating the functionality of loose skins, and with Krogh's principle in mind, we decided to focus on the animal with perhaps the highest looseness index value, the hagfishes (order Myxiniformes). Although most organisms use skin looseness for one or two of these adaptively advantageous functions, hagfishes seem to benefit from all four.

Hagfishes are jawless, benthic marine vertebrates (Miyashita et al. 2019) that possess narrow, elongate bodies and few rigid internal structures. This body morphology in combination with a loose skin grants them the flexibility to tie and manipulate body knots (Haney et al. 2020). Knot tying facilitates feeding on both carcasses and burrowed prey (Zintzen et al. 2011). The skin is loose because hagfishes have a sizeable subdermal blood sinus that accounts for 30% of the total blood volume (Forster 1997). Despite having the lowest blood pressure of all vertebrates, hagfishes have the most blood per unit body mass when compared with other fishes (McDonald et al. 1991; Forster 1998). Several studies (Clark et al. 2016; Boggett et al. 2017; Freedman and Fudge 2017; Haney et al. 2020) have suggested that the resultant disconnect between skin and body core in hagfishes allow for an increased freedom of movement.

Martini (1998) described the scavenging of a whale fall by hagfishes. Hagfishes will create or find an entry into the carcass and begin to use cyclical motions of their unique raspy feeding apparatus to remove a morsel of food. If the tissue upon which they are feeding is unyielding, the hagfish will increase its leverage by forming a knot, manipulating it towards its cranial end, and pressing a loop against the food (Clark and Summers 2012; Clark and Uyeno 2019; Clubb et al. 2019). Of course, a decomposing whale generates a significant concentration of dissolved organic material. Thus, another way of getting nutrients may be to absorb the organic material directly through the skin. Glover and Bucking (2015) note that both juvenile and adult hagfishes are capable of nutrient uptake over the skin. However, the uptake rates of younger hagfishes can be double that of the adults. Thus, the loose skin of hagfishes may represent an increased surface area over which they may absorb nutrients and the younger, skinnier hagfishes, with their relatively higher surface area-to-volume ratio, may be particularly well-suited for this task.

A number of dramatic deep-sea videos taken by Zintzen et al. (2011) show hagfishes being bitten by sharks. Hagfishes are shown to survive initial bites, and then secrete a choking slime into the shark gills. While the sharks are trying to clear their gills, the hagfishes seem to swim away unharmed. This lead Boggett et al. (2017) to hypothesize that hagfish skins are more puncture resistant than those of other fish. However, these investigators found hagfish skins are no more resistant to being pierced by a spring-driven shark's tooth than those of other fish. Because hagfish cores do not fill the entirety of the volume within the skin, Uyeno and Clark (2016) posited that the cores simply are pressed out of the bite path during a shark attack and that no internal damage results. Indeed, Freedman and Fudge (2017) noted that hagfishes are able to move through slit-like apertures that measure less than one-half the body width of the hagfish. Here we consider the contribution of the initial looseness of the skin to the enhancement of overall skin puncture resistance.

Whole body knotting is an impressive biomechanical feat. Hagfishes are not only capable of tying complex knots, but they are able to manipulate the knots anteriorly and posteriorly along their bodies. Hagfishes use these motions to clean their bodies of slime (Adam 1960), to facilitate feeding (Clark and Summers 2012), and to power escape behaviors (Strahan 1963; Hwang et al.

2019; Haney et al. 2020). Interestingly, hagfishes do not appear to use additional slime to lubricate the body surface during knot manipulation. Instead, they may control friction between the skin's inner wall and body core using a mechanism similar to that of mammalian penises or chameleon tongues. The biotribological solution used in these cases involve lubricative sheaths or surfaces that slide easily relative to each other. In the case of the nearly frictionless projection of the chameleon's tongue, de Groot and van Leeuwen (2004) noted that at least 10 slippery sheaths slide relative to each other after the tongue is catapulted out of the mouth.

In assessing the hagfish as a model for studying loose skin function, we begin by describing the anatomy of the skin. Using histological methods, we pay careful attention to the type and orientation of muscle and connective tissue fibers. We investigated two species of hagfishes, the Pacific hagfish (*Eptatretus stoutii* (Lockington, 1879)) and the Atlantic hagfish (*Myxine glutinosa* Linnaeus, 1758), in an effort to document some of the diversity found in hagfish skins. Furthermore, these two species are members of the two important subfamilies of hagfishes (Eptatretinae and Myxininae) that collectively contain approximately 90% of all hagfish species (Fernholm et al. 2013). Second, to assess the effect of increased structural extensibility during biting attacks, we perform standardized puncture tests, developed by the American Society for Testing and Materials, on skin samples of both hagfish species as well as the tight-fitting anguilliform skin of *A. rostrata*. Samples of skins from all species were tested while preloaded in tension (representing the tight-fitting morphology) and while unstressed (representing the loose-fitting morphology). Third, we physically model the sheath–core organization of the hagfish skin and body. This analysis is important because it has already been shown that nearly three-quarters of the overall body stiffness of a hagfish is attributed to their notochords, whereas their loose skin contributes little (Long et al. 2002*a*, 2002*b*). The relationship between skin tension and forces experienced in the notorchordal core of the hagfish body depends on the pressure of the hemocoel. Therefore, this pressure may contribute to the fine-tuning of overall body stiffness and affect the ability to perform body knots of various configurations.

Materials and methods

The following animal use protocols were approved by Valdosta State University's Institutional Animal Care and Use Committee (Protocol AUP-00054-2017).

Histology

Five specimens of *E. stoutii* and five specimens of *M. glutinosa* were used in this study. Live specimens of *E. stoutii* were provided by the Washington Department of Fish and Wildlife and Olympic Coast Seafoods LLC (Port Angeles, Washington, USA) and live specimens of *M. glutinosa* were collected at Shoals Marine Laboratory (Appledore Island, Maine, USA). All specimens were shipped to, and housed at, Valdosta State University. Specimens were euthanized using 400 mg MS222 (Finquel anaesthetic; Argent Chemicals, Redmond, Washington, USA) and 200 mg $NaHCO_3$ (pH buffer) mixed in 1 L of seawater. The skin samples were dissected out and were then fixed for 48 h in 10% neutral-buffered formalin. The fixed tissues were then cut into a series of 5 mm × 10 mm segments for histological paraffin infiltration using cassettes. Orientation was preserved at each step to facilitate subsequent analyses. These tissue segments were then dehydrated in a series of ethanol (ETOH) baths. Tissue segments were run for 2 h in each bath in the following sequence: (1) 15% ETOH, (2) 30% ETOH, (3) 45% ETOH, (4) 60% ETOH, (5) 75% ETOH, (6) 90% ETOH, and (7) 100% ETOH. Skin samples were then bathed for 2 h in a 50% absolute ETOH and 50% CitriSolv solution (Deacon Labs, Inc., King of Prussia, Pennsylvania, USA), followed by 2 h in 100% Citri-Solv, to facilitate the infiltration of liquid paraffin (Paraplast

Fig. 2. Methods for measuring the morphological and mechanical characteristics of hagfish skins. (A) Sampling, embedding, and sectioning of skin samples. Sections were positioned together in a paraffin block at mutually perpendicular orientations so that transverse (A. Trans.) and longitudinal (B. Long.) sections were produced. (B–C) Photographs of vertical motorized testing stand equipped with a standard ASTM F1306 puncture testing apparatus. Puncture data were collected from tests performed on both loose (B) and taut (C) samples of skins dissected from American eels (*Anguilla rostrata*), Atlantic hagfishes (*Myxine glutinosa*), and Pacific hagfishes (*Eptatretus stoutii*). Note in B and C, the left photographs show samples of skin prior to running a test, whereas the right photographs are of the samples after they were punctured.
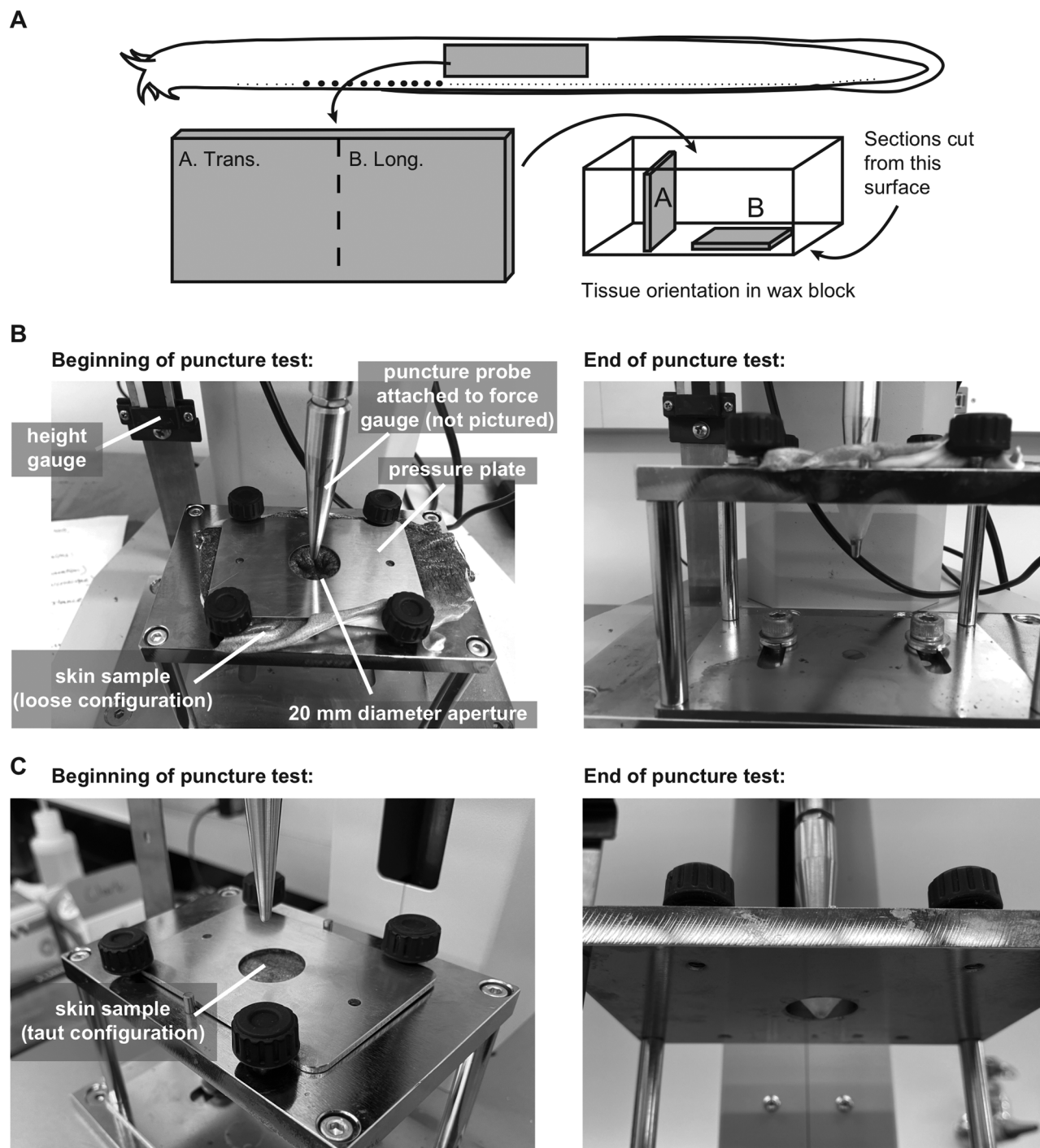
Plus, Leica Biosystems, St. Louis, Missouri, USA) during a series of three 1 h paraffin baths under vacuum. Paraffin-infiltrated tissues were then embedded into wax blocks for sectioning. Wax blocks were cut and faced, and a Finesse ME+ Microtome (Thermo Scientific, Waltham, Massachusetts, USA) was used to cut 10 μm thick sections in both longitudinal and transverse orientations (Fig. 2A) Collected sections were placed in a 46 °C water bath for approximately 5 min to expand and remove cutting distortions.

Sections were then placed on slides prepared with Mayer's albumin and heat fixed on a 43 °C hot plate overnight (Kier 1992). A modified Milligan's trichrome staining protocol (Kier 1992) was used to differentiate between three tissue types; muscle tissue stained magenta, connective tissue appeared blue, and blood cells stained orange. The staining process was carried out using a Gemini AS automated slide stainer (Thermo Scientific, Waltham, Massachusetts, USA). Cover slips were then affixed to the stained slides using Permount (Fisher Chemical, Waltham, Massachusetts, USA). The sections were visualized using transmitted and phase-contrast light microscopy (the latter was used to enhance the pattern of fiber orientation).

Puncture testing

To test the effect of skin looseness on puncture resistance, we relied on a standardized puncture test, the ASTM F1306 protocol (ASTM 1990). This industrial technique was designed to measure and compare puncture resistance across a diversity of synthetic and biological films and sheets. The test measures puncture resistance (the applied force at failure) and puncture distance (the distance traveled at failure) as a ball-ended conical probe is pressed, at a rate of 25 mm/min, through a sample of material held within a circular frame with a diameter of 20 mm (Figs. 2B and 2C). We adopted this technique because of the following. (1) It is slow enough that one can ignore the overall effect of the force acting over time (impulse). (2) The ball probe was designed to apply force over a standardized area so that material failure that results in puncture is consistent. The blunt ASTM F1306 puncture probe is particularly useful for comparative tests, whereas sharp probes with edges add other variables by concentrating forces and cutting fibrous material on contact (e.g., Boggett et al. 2017). (3) The suspensory testing frame allowed for the sample material to be mounted with a controlled measure of tension that reflects taut versus loose skins.

For taut skin tests, the sample held within the frame measured 38.1 mm^2 and was held in place without any sagging (Fig. 2C). For the loose skin tests, the sample measured 76.2 mm^2 and was held in place such that twice the area of tissue was suspended within the 20 mm diameter circular frame (Fig. 2B). This configuration for skin samples created a looseness that added 15 mm of distance through which the probe had to move the skin prior to putting it into tension. Fresh skins were tested from three species — five individuals of *E. stoutii* (5 loose samples, 5 taut samples), four individuals of *M. glutinosa* (1 loose sample, 4 taut samples), and four individuals of *A. rostrata* (4 loose samples, 6 taut samples). In both loose and taut treatments, we measured (*i*) initial skin thickness (L_{0T}), (*ii*) the applied force at puncture (puncture force), (*iii*) the distance traveled from contact to puncture (puncture distance; ΔL), and (*iv*) the energy delivered by the probe or the energy absorbed by the skin sample at puncture (puncture energy) that was measured as the integral of puncture force–distance traces.

To account for intraspecific and interspecific differences in the skins, puncture force and puncture distance were converted to puncture stress and a normalized puncture distance (NPD). Puncture strength, the puncture stress applied at failure, was calculated by dividing the applied force by the surface area of the probe tip (63.34 mm^2). The unitless variable NPD ($\Delta L/L_{0T}$) equaled the change in puncture distance (ΔL, mm) divided by the unloaded skin sample's thickness (L_{0T}, mm). Although different from the usual mechanical strain calculation, our equation for NPD provided a standardized measure of probe travel distance to help validate the comparisons of puncture mechanics between species and between preset levels of tension. We used this alternative metric because it allowed us to compare loose skin that was extending while still not under measureable tension with tests done of taut skin. We also standardized puncture energy measurements by calculating the integral of puncture stress–NPD curves, which we call normalized puncture energy per unit volume (NPE).

All data sets met normality following Shapiro–Wilk's tests. Student's *t* tests with Bonferroni corrections were then used for comparing mean data between species and between skin treatments (loose and taut). Mean data were initially compared between *M. glutinosa* and *E. stoutii* skins. These data were then pooled for subsequent comparisons with *A. rostrata* puncture data. Mean puncture force, puncture strength, puncture distance, NPD, puncture energy, and NPE were compared between species. These data were also compared between loose and taut treatments per species. We also compared mean thickness of the skins from *E. stoutii* and *M. glutinosa*. All statistical analyses were done in JMP Pro version 14 and $p < 0.025$ was used as the criterion for significance.

Physical modeling

Our simple model used a length of 150# test monofilament fishing line as a "notochord". The nylon filament had a memory, or set, and coiled when not under tension. The line was tied within a 5 cm diameter 260Q latex twisting balloon (the type used for twisting balloon animals and sculptures). Although the maximum diameter was inherent to the type of balloon, we were able to set the maximum length of the structure by selecting the length of the fishing line. Haney et al. 2020 compared the length-to-width aspect ratios theoretically required to form various types of knots that hagfishes are known to tie and the actual ratios measured from hagfishes. The two knots that hagfishes most readily favor are overhand and figure-8 knots. Overhand knots require a relatively short aspect ratio of 16.37, whereas figure-8 knots require a relatively longer ratio of 21.05. Haney et al. 2020 reported mean length-to-width ratios of 22.41 for *E. stoutii* and 28.58 for the relatively skinnier *M. glutinosa*. Thus, we set the fishing-line "notochord" length to a biologically appropriate 120 cm to give an aspect ratio of 24 (Fig. 3). This aspect ratio was long enough to tie both overhand and figure-8 knots and was close to the mean values exhibited by myxinines and eptatretines.

The physical model (Fig. 3) was built by tying a stopper knot at both ends of the fishing line. The line was then threaded through the neck and lumen of the balloon. The end of the balloon was whipped with several turns of dental floss so that the stopper knot could not be pulled back through the balloon. The whipping turns were placed at such a point along the balloon so that when inflated the balloon would be roughly the same length as the fishing line (this left a small length of unused balloon at the end). The neck of the balloon, with the proximal stopper knot extending from it, was stretched over the male luer lock fitting of a three-way stopcock. The balloon and fishing line were securely affixed to the luer fitting with several more turns of dental floss. The stopcock had two female luer ports; to these we attached two custom built adaptors made from syringe barrels. The syringe barrel attached to the inline female port had a sports ball inflation needle with a Schrader valve stem epoxied within and a 22-gauge hypodermic needle was epoxied into the barrel attached to the side female port. The hypodermic needle served as a port through which an optical pressure sensor (An OPP-M pressure sensor attached to a LifeSens single channel signal conditioner; OpSens Solutions, Québec, Quebec, Canada) could be inserted and made airtight using modeling clay. The connector of a portable electric (12 VDC, 2 A) tire pump was attached to the inflation needle and used to pump up the balloon to various pressures as recorded by the pressure sensor. A camera (Sony α7 S DSLR/FE 28–70 mm lens) was used to video record the balloon and pressure sensor as it inflated and deflated. The stopcock allowed us to stop the inflation or deflation to attempt to tie knots into the balloon at various pressures.

Results

Histology

Histological sections of the dermis from *E. stoutii* skins possessed components that had either the staining characteristics of

Fig. 3. Custom experimental rig for testing physical models of hagfish bodies. Inset to the left shows how air travels from the air pump hose to the balloon and to the pressure sensor. The inset to the right shows how dental floss was used for tying off the fishing line (the "notochord") at the distal end of the balloon (the "skin"). Note the progressive straightening of the fishing lure as the balloon is being pressurized and inflated.
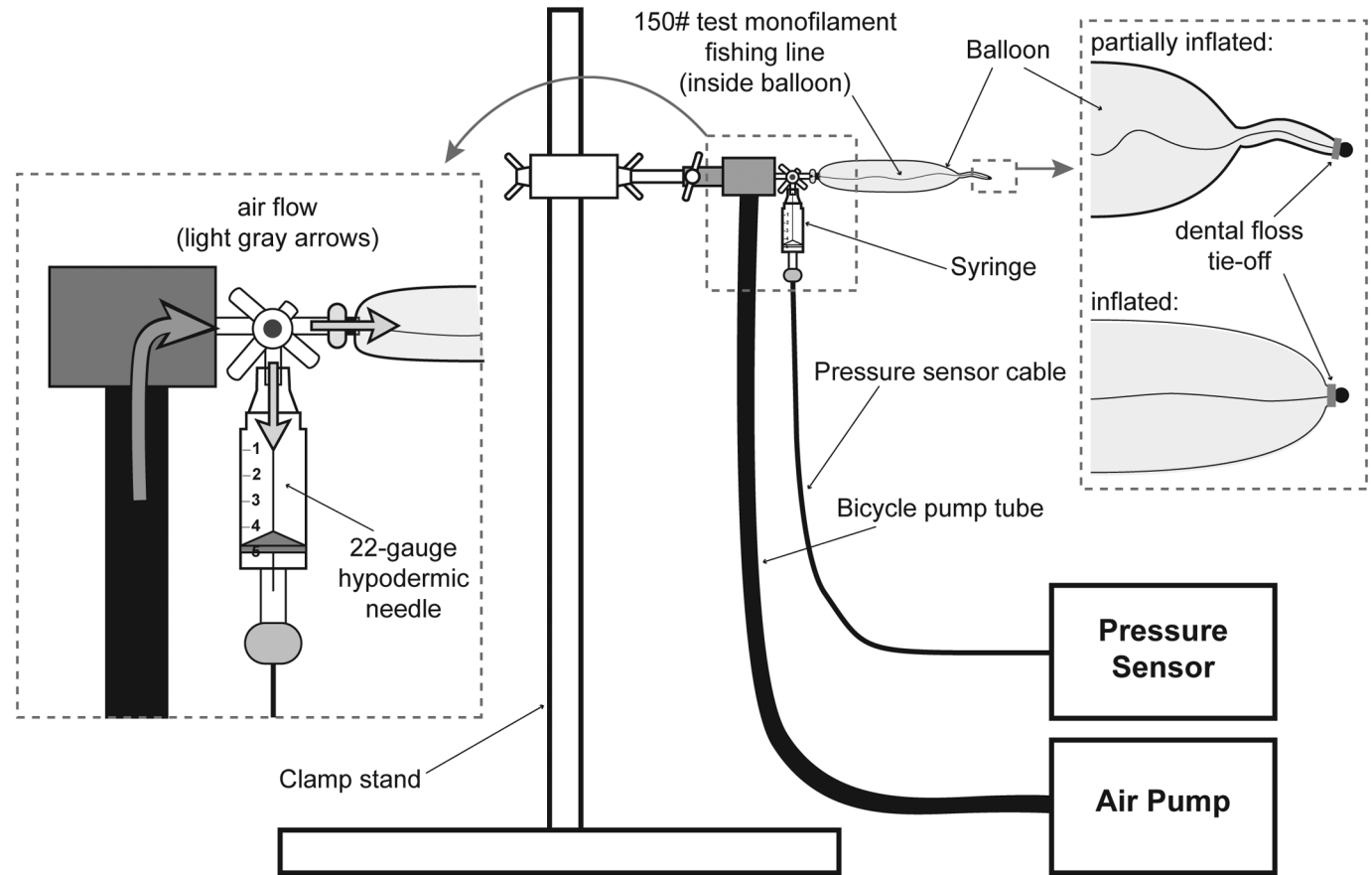
muscle (magenta) or the connective tissue (blue) (Fig. 4A). In contrast, the components of the dermis from *M. glutinosa* skins only stained like connective tissue (blue) (Fig. 4B). Grazing parasagittal sections show that the fibers contained in the dermis of *E. stoutii* skins were wavy, in contrast to the straighter fibers in *M. glutinosa*. Despite these differences, mean angle measurements of grazing skin sections of *E. stoutii* (46.4°, SD = 4.07°, $n = 4$) and *M. glutinosa* (43.7°, SD = 2.23°, $n = 2$) were quite similar and ranged from 40° to 51° across all specimens. Prior to histology, fresh skin measurements showed that those from *E. stoutii* were thicker than those from *M. glutinosa*. Mean thickness of *E. stoutii* skins (0.603 ± 0.02 mm, mean ± SE) and *M. glutinosa* skins (0.495 ± 0.02 mm) were significantly different ($p < 0.0005$). Collectively, the skins of *E. stoutii* and *M. glutinosa* were less than 50% of the mean thickness of *A. rostrata* skins (1.332 ± 0.14 mm).

Puncture testing

The ASTM F1306 protocol allowed us to differentiate the puncture resistance between individuals of the three species (Figs. 5A and 5B). All skins initially exhibited J-shaped puncture force–distance and stress–NPD traces, with a curvy toe region followed by a steeper and substantially more linear slope. Immediately prior to failure, some samples (in representatives of *A. rostrata* and *E. stoutii*) show a slight decrease in slope (Fig. 5A and 5B). Relative to taut skins in all species, the onset of tension in the loose skins was shifted to the right (Figs. 5A and 5B) because the probe

needed to travel approximately 15 mm before placing the loose skins into tension.

There were significant differences between *E. stoutii* and *M. glutinosa* and *A. rostrata* in virtually all parameters of skin puncture mechanics (Table 2); however, these data were similar between taut and loose samples of skins within the hagfishes and within the *A. rostrata* (Table 3). Our data show that *A. rostrata* skins are at least five times more puncture resistant than the skins from both hagfishes, which, themselves, exhibited similar puncture resistance (Fig. 5A). In both taut and loose treatments, skins from *A. rostrata* required significantly larger magnitudes of force ($p < 0.0001$) to achieve puncture (Table 2). When puncture forces were normalized by the surface area of the puncture probe's tip, taut treatments of *A. rostrata* skins (2.41 ± 0.23 MPa, mean ± SE) required more than five times the puncture stresses applied to *M. glutinosa* skins (0.44 ± 0.19 MPa) and over six times the puncture stresses on *E. stoutii* skins (0.38 ± 0.04 MPa; Fig. 5B). Both taut and loose treatments of *A. rostrata* skins resisted significantly greater magnitudes of puncture stress than hagfish skins (Table 2).

NPD from taut and loose treatments of hagfish skins were significantly greater than the NPD of *A. rostrata* skins ($p < 0.0001$ in taut samples and $p < 0.0004$ in loose samples; Table 2 and Fig. 6A). At 16.5 ± 0.78 and 18.8 ± 1.63 in *E. stoutii* and *M. glutinosa*, respectively, the NPD of taut samples from hagfish skins were 1.6–1.8 times greater than the NPD of *A. rostrata* skins (10.5 ± 0.93). The mean NPD required to puncture loose treatments of the skins

Fig. 4. Light micrographs of hagfish skin histological preparations. (A, top) Transverse section of the skins from a Pacific hagfish (*Eptatretus stoutii*) on the left and an Atlantic hagfish (*Myxine glutinosa*) on the right with measurements of the thickness of the dermis. (A, bottom) Grazing parasagittal sections of skins from *E. stoutii* and *M. glutinosa*. All samples examined in A were stained with a modified Milligan's trichrome protocol to visualize and distinguish muscle (magenta) and collagen (blue). (B) Hematoxylin and eosin stained transverse section of an *E. stoutii* skin sample (left) with a close up view of the fibrous dermis (right). (C) Transverse section of an *E. stoutii* skin sample stained with Verhoeff – Van Gieson stain (left) to demonstrate the presence of both elastin (black) and collagen (red) fibers. Due to limited field access to sample and stain, the *M. glutinosa* skin sample (right) was only processed using Verhoeff stain, without counterstain, to show only elastin fibers within the dermis.
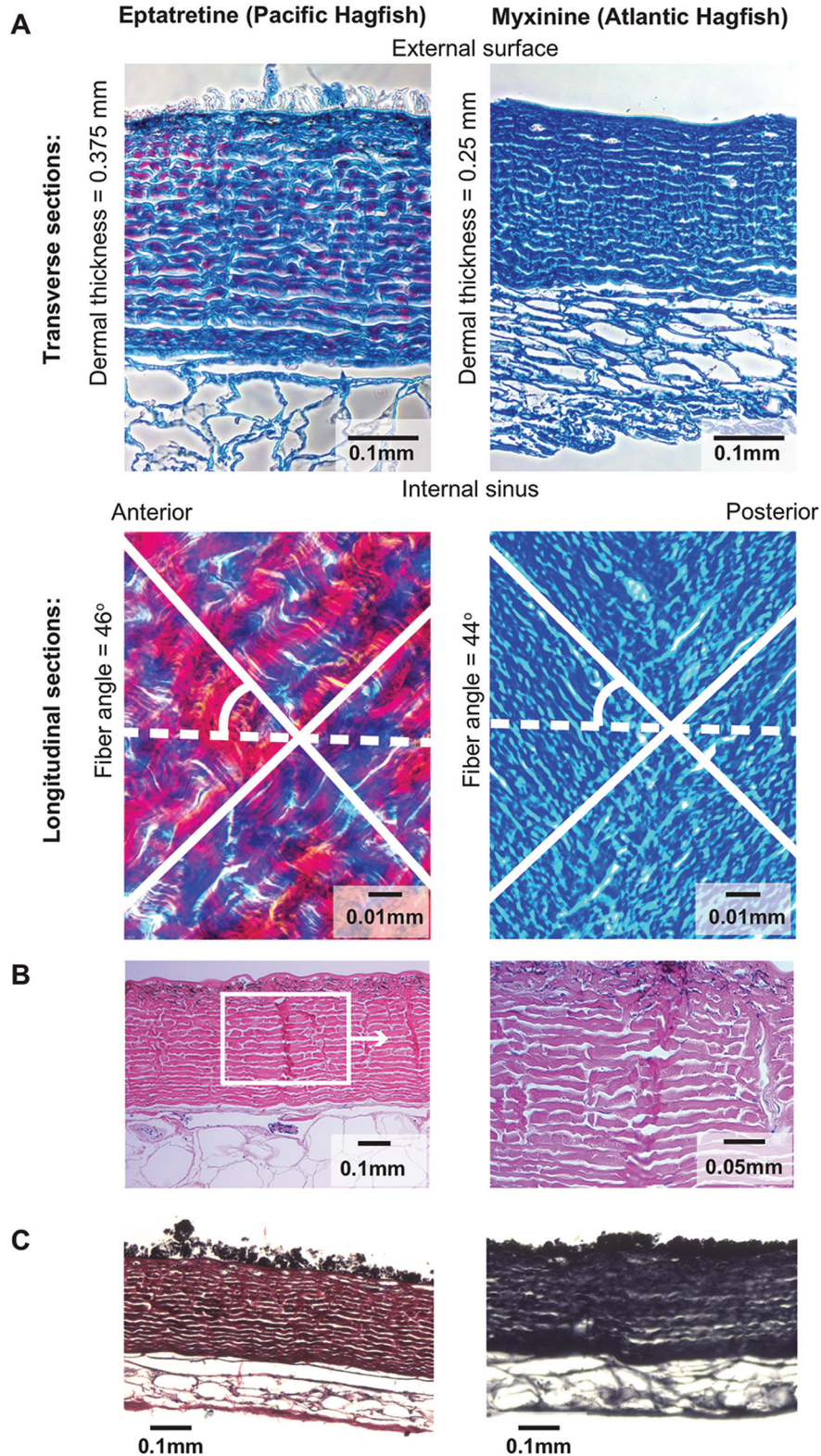
Fig. 5. Puncture force–distance traces from American eels (*Anguilla rostrata*), Atlantic hagfishes (*Myxine glutinosa*), and Pacific hagfishes (*Eptatretus stoutii*). Traces of each species are dashed or solid and shape coded. (A) Raw puncture force–distance traces from the individual skin samples tested from taut and loose treatments. Note the variation and clustering of data across individuals of a species. (B) Raw puncture stress – normalized puncture distance (NPD; $\Delta L/L_{0T}$) curves from loose and taut treatments of *A. rostrata*, *M. glutinosa*, and *E. stoutii*.
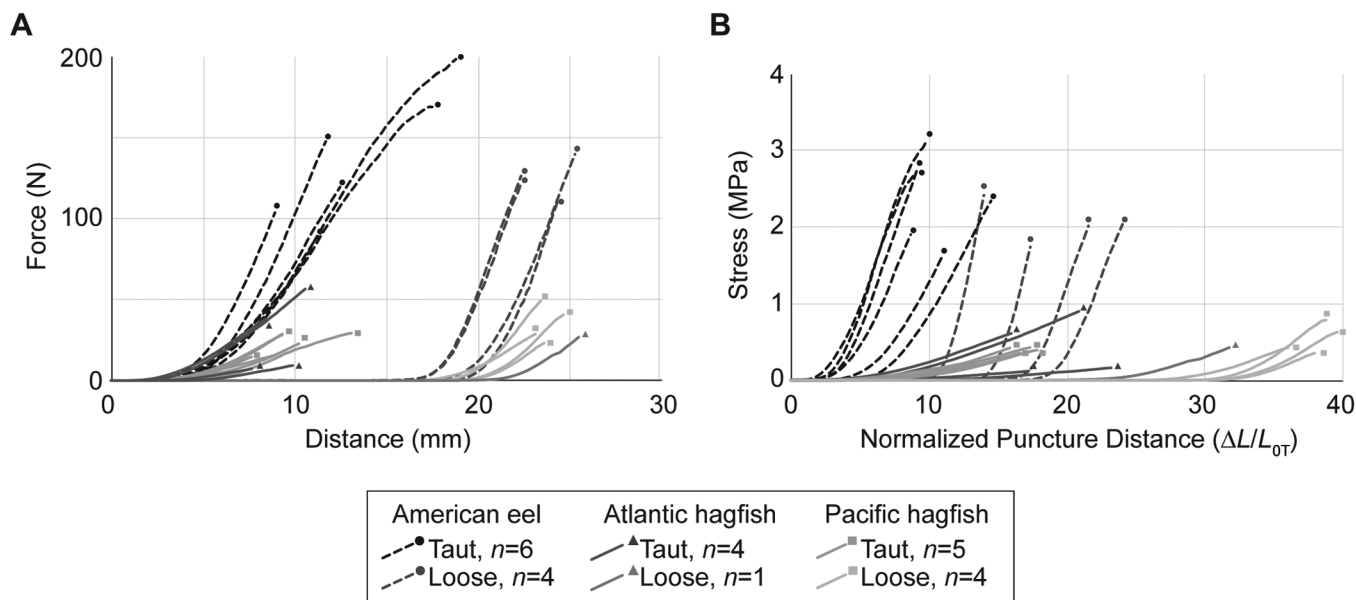
Table 2. Comparative puncture mechanics in the skins of hagfishes (pooled data from Pacific hagfish (*Eptatretus stoutii*) and Atlantic hagfish (*Myxine glutinosa*)) and American eels (*Anguilla rostrata*).

Variable	Hagfishes	American eel	p
Taut skin samples			
Puncture force (N)	24.7 ± 7.40	137 ± 19.8	**<0.0001**
Puncture strength (MPa)	0.41 ± 0.11	2.41 ± 0.23	**<0.0001**
Puncture distance (mm)	9.44 ± 6.40	13.1 ± 1.73	**0.0165**
Normalized puncture distance	17.6 ± 1.20	10.5 ± 0.92	**<0.0001**
Puncture energy (J)	0.11 ± 0.03	0.58 ± 0.15	**<0.0009**
Puncture toughness (MJ·m^{-3})	2.13 ± 0.71	7.79 ± 1.11	**<0.0002**
Loose skin samples			
Puncture force (N)	30.5 ± 4.85	127 ± 6.20	**<0.0001**
Puncture strength (MPa)	0.49 ± 0.10	2.00 ± 0.10	**<0.0001**
Puncture distance (mm)	24.6 ± 0.29	23.4 ± 0.74	0.5446
Normalized puncture distance	34.7 ± 1.03	19.5 ± 2.33	**0.0004**
Puncture energy (J)	0.07 ± 0.01	0.28 ± 0.03	0.4953
Puncture toughness (MJ·m^{-3})	1.74 ± 0.40	3.75 ± 0.58	**0.0094**

Note: Data are means ± SE. Values in boldface type indicate $p < 0.025$.

Table 3. Differences in the puncture mechanics between taut and loose skin samples from hagfishes (pooled data from Pacific hagfish (*Eptatretus stoutii*) and (*Myxine glutinosa*)) and American eels (*Anguilla rostrata*).

Variable	Taut	Loose	p
Hagfishes			
Puncture force (N)	24.7 ± 7.40	30.5 ± 4.85	0.253
Puncture strength (MPa)	0.41 ± 0.11	0.49 ± 0.10	0.327
Puncture distance (mm)	9.44 ± 6.40	24.6 ± 0.29	**<0.0001**
Normalized puncture distance	17.6 ± 1.20	34.7 ± 1.03	**<0.0001**
Puncture energy (J)	0.11 ± 0.03	0.07 ± 0.01	0.172
Puncture toughness (MJ·m^{-3})	2.13 ± 0.71	1.74 ± 0.40	0.510
American eel			
Puncture force (N)	137 ± 19.8	127 ± 6.20	0.640
Puncture strength (MPa)	2.41 ± 0.23	2.00 ± 0.10	0.204
Puncture distance (mm)	13.1 ± 1.73	23.4 ± 0.74	**0.0015**
Normalized puncture distance	10.5 ± 0.92	19.5 ± 2.33	**0.0032**
Puncture energy (J)	0.58 ± 0.15	0.28 ± 0.03	0.063
Puncture toughness (MJ·m^{-3})	7.79 ± 1.11	3.75 ± 0.58	0.025

Note: Data are means ± SE. Values in boldface type indicate $p < 0.025$.

from *E. stoutii* (38.4 ± 1.03) and *M. glutinosa* (31.0) were 1.6 times greater than that required to puncture loose treatments of *A. rostrata* skins, which punctured at normalized distances of 19.5 ± 2.33 (Fig. 6A). However, in realistic biological settings, a more proper comparison of the NPDs might be drawn between taut treatments of *A. rostrata* skins and loose treatments of the hagfish skins. Under these conditions, the loose samples of hagfish skins (31–38) punctured at normalized distances roughly three to four times the NPDs applied to *A. rostrata* skins (Table 2 and Fig. 6A).

NPE was significantly greater in both taut and loose samples of *A. rostrata* skins than in taut and loose samples of hagfish skins ($p < 0.0002$ in taut treatments and $p = 0.0094$ in loose treatments; Table 2). Taut samples of *A. rostrata* skins stored three to four times

more normalized energy prior to puncture (7.79 ± 1.11 MJ·m^{-3}) than taut skins from *M. glutinosa* (2.50 ± 1.22 MJ·m^{-3}) and *E. stoutii* (1.76 ± 0.20 MJ·m^{-3}; Fig. 6B). Loose treatments of *A. rostrata* skins required approximately 1.8–2.4 times more NPE (3.75 ± 0.58 MJ·m^{-3}) than loose samples of *M. glutinosa* (1.57 MJ·m^{-3}) and *E. stoutii* (1.91 ± 0.40 MJ·m^{-3}; Fig. 6B).

Pressurization of a sheath that is limited in length by an internal core

The balloon was inflated slowly from 0 kPa to its bursting point of 18 kPa (Figs. 7A–7E). Throughout this range, there were four distinct stages delineated by the relationship between the flexible notochord-like core and the inflatable balloon sheath:

Fig. 6. Puncture stress and normalized puncture distance (NPD; $\Delta L/L_{0T}$) data. (A) Mean stress and NPD data measured from loose (grey) and taut (black) treatments of the skins from American eels (*Anguilla rostrata*) (circle markers), Atlantic hagfishes (*Myxine glutinosa*) (triangle markers), and Pacific hagfishes (*Eptatretus stoutii*) (square markers). (B) Normalized puncture energy (NPE) required to puncture loose (grey) and taut (black) treatments of fish skins. The data in both graphs are means ± SE.
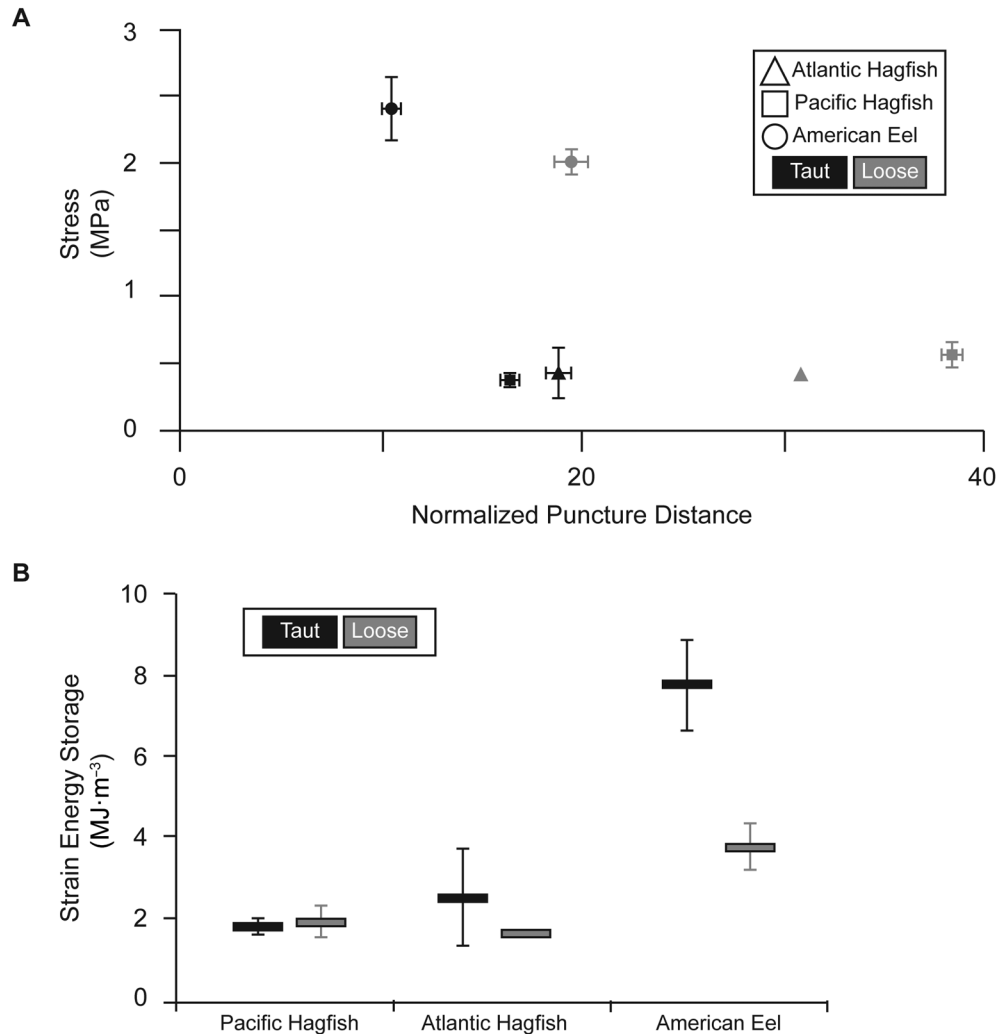
1. At very low pressures that measured less than 15% of burst strength (e.g., 1 kPa; Fig. 7A), there was not enough volume of air to completely inflate the balloon. As such, because the uninflated length of the balloon was shorter than the length of the core, the structure took on a coiled shape in which the balloon was stretched between loops of the fishing-line core.

2. At 17% of burst strength (3 kPa; Fig. 7Bi), the balloon was inflated and the internal pressure allowed for enough turgidity to support its own mass when held horizontally. However, the fishing-line core was not in tension and formed loose loops within the lumen of the balloon. The core often came into contact with the balloon. At this pressure, the balloon was flexible enough that one could tie a loose figure-8 knot with it without any kinks forming (Fig. 7Bii).

3. At 56% of burst strength (10 kPa; Fig. 7Ci), the internal core was held away from the walls of the balloon but still showed slight coiling, and thus presumably was under very little tension. There was increase structural support from the

balloon's turgor; however, the structure became stiff enough that a figure-8 knot could no longer be tied without the balloon kinking. The simpler overhand knot could be loosely tied without kinking (Fig. 7Cii).

4. At pressures from 78% to 100% of burst strength (14–18 kPa; Figs. 7Di and 7E), the balloon became increasingly turgid. Because the sheath was limited in length by the internal fishing-line core, the fishing line was held straight in tension while the sheath increased in diameter and began to form a sinusoidal curve. This bowing away from the tensile core was caused by lateral expansion of the balloon en lieu of elongation. At these pressures, it became difficult to even bend the balloon without causing it to kink (Fig. 7Dii).

Discussion

Histological analyses of hagfish skin

In comparing the skins of *E. stoutii* and *M. glutinosa*, we can document the anatomical diversity between the skins of the two

Fig. 7. Photographs of changes in shape and flexibility of a balloon sheath and fishing-line core model at various inflation pressures. Images on the left (A–E) show increasing pressures from 1 to 18 kPa (burst pressure). Images on the right (Bii–Dii) show inflated balloon models at various non-destructive pressures and the relative changes in flexibility. Note that at the highest non-destructive pressure (Dii), the model can be bent but is incapable of being knotted and the fishing-line core within is under tension. Knots begin to be able to be formed only at pressures where the fishing-line core is no longer taut. With decreasing pressures, knots of increasing complexity can be formed (Cii shows an overhand knot being tied at 10 kPa, and only at 3 kPa (Bii) can a figure-8 knot be tied).
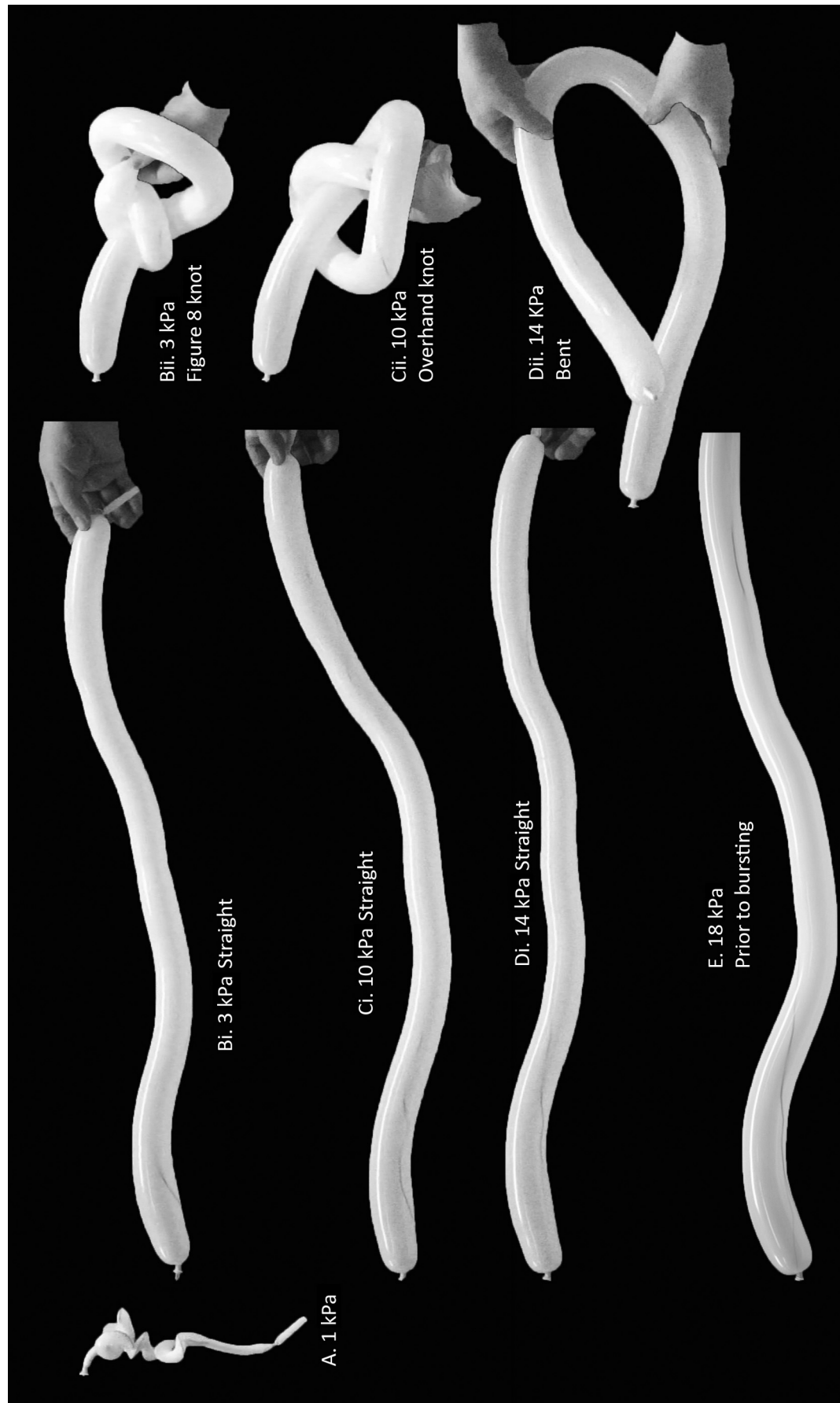
major lineages (subfamilies Eptatretinae and Myxininae). We find some considerable differences and commonalities:

1. When normalized to body diameter, *E. stoutii* has thicker skin (0.547 ± 0.03 mm (mean ± SE), *n* = 5 animals) than *M. glutinosa* (0.457 ± 0.02 mm, *n* = 5 animals). Furthermore, the dermises of *E. stoutii* skins contain more and thicker fibers (mean = 26 layers, SD = 7.116 layers, *n* = 5) than the dermis of in *M. glutinosa* skins (mean = 18 layers, SD = 1.41 layers, *n* = 4). Despite this difference in skin thickness, Haney et al. 2020 found that *E. stoutii* tend to form relatively tighter body bends than does *M. glutinosa*.

2. Nearly all of the fibers in the skin of *M. glutinosa* stain in a manner consistent with collagen (Fig. 4A, right, blue). This is not true for *E. stoutii* skins in which the dermal layer is invested with additional inclusions that stain like muscle (Fig. 4A, left, magenta). Initially, we considered that this suggested potentially "active" and "non-active" integuments, with implications for functional differences in body motion between these two skins. However, two quick follow-up investigations suggest that eptatretine hagfish skin does not contain active musculature: Hematoxylin and eosin staining of *E. stoutii* skin sections indicate that the magenta fibers do not have many nuclei and are thus not likely muscle fibers (Fig. 4B). Also, electrical simulation trains applied to fresh skin using field electrodes did not elicit contractions as they did in body wall musculature. Much of the passive elasticity of hagfish skins may, in addition to collagen, be due to a heavy presence of elastin as confirmed in paraffin sections made of a single *E. stoutii* specimen using Verhoeff – Van Gieson stain and, due to limited field access to sample and stain, a single *M. glutinosa* skin using only Verhoeff stain for elastin (Fig. 4C).

3. The dermis of both hagfish species are composed of 16–39 layers of crossed helical fibers. In grazing sections (Fig. 4A, longitudinal sections), the fibers were found to be oriented at roughly a 45° angle to the long axis of the body (halfway between longitudinally arranged (0°) and hoopwise (90°) fibers). Although this angle, less than 54.7° (Clark and Cowey 1958), suggests that the subdermal sinus is either capable of great deformations in widths or lengths or increasing in volume before these connective tissue fibers are put into tension, the notochord limits the length of the animal. As such, the skin, with its fixed angular mean value of 45° between the opposing helically wound connective tissue fibers, acts like a piece of bias-cut cloth (cut 45° to the warp and weft threads and major seams). Such pieces of woven fabric are more elastic and fluid when sheared in the bias direction compared with straight and cross woven cloth (Domskienè and Strazdienè 2005). This shearing behavior allows for maximal deformation, and therefore structural extensibility, during a puncture attack. This ability of the skin to deform is enhanced by the relatively flaccid nature of the skin.

Puncture resistance

To successfully puncture a skin or membrane, the dentition or puncture probe must first place the membrane into tension. This tension is loaded quickly upon contact with a taut membrane; however, there is a delayed loading if the membrane is loose. This is because the probe must first travel the distance to remove slack before beginning to generate tension. Once stretched taut, force can then be applied until a critical amount of tension is reached and puncture is achieved. In all species of fish that we examined, loose skin treatments exhibited force–distance traces with higher slopes than their respective taut skin treatments (Figs. 5A and 5B). In natural settings, hagfish skins are likely subjected to biting assaults that cover less distance and fail to deliver the required force to induce puncture than in experimental conditions. This discrepancy might imply a safety factor (Vogel 2013) possessed by hagfish skins. Hagfishes rely on slime as a secondary line of defense from biting assaults, and upon contact, is rapidly secreted and may clog the gills of the attacker (Lim et al. 2006; Zintzen et al. 2011).

Immediately prior to failure, some samples from each species show a relatively inconspicuous decrease in slope reminiscent to the yield points along force–distance curves, though declining slopes were absent in some of these curves (Fig. 5A). This analogous yield point along the force–distance curves may represent the puncture force and distance where the sample is permanently deformed. At these moments, the probe may be nearing the interior edge of the dermis, which must be breached to see the characteristic drop in force once puncture is achieved. Under standard conditions, hagfish skins require significantly less force to puncture than *A. rostrata* skins (Figs. 5A, 5B, 6A, and 6B). These results corroborate the hypothesis that the puncture resistance of *E. stoutii* and *M. glutinosa* skins is not extraordinary (sensu Boggett et al. 2017), but they also demonstrate that the puncture resistance of hagfish skins may occur in the lower end of the range in puncture resistance across other fish skins. Indeed, additional ASTM F1306 puncture tests on the skins of more species are needed to address this. Nonetheless, the significantly lower puncture forces and stresses coupled with the absence of scales present the possibility that the skins of hagfishes might be among the least puncture resistant of fish skins.

Despite being less resistant to applied puncture forces and puncture stresses, the skins of hagfishes benefit from proportionately longer puncture distances than *A. rostrata* skins. NPDs in taut and loose treatments of hagfish skins are nearly twice that in *A. rostrata* skins (Table 2; Figs. 6A and 6B). Hagfish skin appears puncture resistant because its looseness increases the distance that the probe or tooth must travel through to do harm. Hagfish skins require almost twice the distance (188%) and strain to puncture (198%) than that of *A. rostrata* skins when considering realistic functional situations reminiscent of comparing taut treatments of *A. rostrata* skin with loose treatments of hagfish skin.

The tight-fitting appearance of the skins from teleosts like *A. rostrata* results from intricate myoseptal–skin connections between the skin and the core (Danos et al. 2008). These morphologies impose a preliminary "resting" tensile stress on intact skins, and they result in a shorter distance required for puncture. The body core tissues of the teleost become punctured immediately after the tooth tip breaches the inner surface of the skin. In the hagfishes, a substantial amount of decoupling of the body core and skin creates a longer bite path required for puncture. This strategy seems akin to "pre-de-stressing" the material prior to assault and provides the hagfish body covering with a high degree of puncture distance that must be overcome to effectively harm underlying tissues. By increasing puncture resistance through looseness, hagfishes are able to persist with smooth, scale-less, skins with large surface areas that possibly facilitate other skin requirements such as nutrient uptake (Glover et al. 2011) and the flexibility required for knotting (Clark et al. 2016) and squeezing through small spaces (Freedman and Fudge 2017).

We also note that loose samples of *A. rostrata* skins required half the amount of energy to puncture than taut skins. In other words, the areas under the puncture traces from loose *A. rostrata* skins were smaller than the areas under the taut skin puncture traces. The reason for this discrepancy between these treatments is possibly geometrical; during the course of a puncture test (post-contact), the angle between the probe and the skin sample progressively becomes more acute as the probe travels along its puncture path. These changes create larger vertical components of the applied puncture force that would normally be smaller in magnitude when testing a taut sample.

Physical simulations with balloons

Two interesting phenomena arise from the balloon model. First, no useful bending can occur at any pressure where the nylon line core "notochord" in under tension. As such, knotting only occurs when the tension in the balloon "skin" is lower (i.e., lower pressure) and the filament "notochord" is in compression and can be seen starting to coil within the balloon. Second, the radii of loops that can be formed without kinking (local buckling) become tighter as the internal pressure and tension in the "skin" drops. Thus, this model corroborates findings that notochords are likely used for axial stiffness and built to bear compression (Long et al. 2002b). Additionally, the loosely connected "notochord" need not stay at the center of the balloon's cavity "blood sinus"; during loop formation, stiffness of the "notochord" causes the fishing line to be repositioned towards the outer edge of the bend. This ability to reposition the core within the sinus may be biologically beneficial when skins are being punctured, such as during a shark attack (Boggett et al. 2017).

Pieranski et al. (2001) noted that for maximally tightened knots, the more complex the knot, the larger the radii of the constituent loops. Their physical and virtual models showed that loops of larger radii tend to contribute less to pinch points and thus reduce internal stresses. Thus, one might assume that balloons bearing knots that are more complex would withstand the highest internal pressures. However, we found the tying of a complex figure-8 knot (rather than a simpler overhand knot) to be possible only in balloons inflated with low pressure. This is because only in maximally tightened knots do simpler knots take less length. If body stiffness limits the minimal radius of possible curvatures, then the amount of body length required to tie a knot increases. Thus, at higher pressures, overhand knots are easier to tie because they have fewer loops of larger radii that can be tied into a stiffer body (Fig. 7Ci and 7Cii). Of course, in real hagfishes, the pressure of the subdermal sinus is always low, reaching only 0.147 mm Hg (20 Pa) (Satchell 1984), which is significantly less than an aortic pressure of 3–8 mm Hg (400–1067 Pa) (Wright 1984).

Broad conclusions

Loose hagfish skins may be an ideal model in which to study the functionality of loose skins in general. This is because our analysis suggests a number of testable postulates for the function of loose skins in hagfishes. Skin looseness may provide the freedom of movement required to form body loops of short radii and, coupled with the smooth scale-less epidermis, provides a slick surface that allows sliding within formed knots. Haney et al. (2020) provides an initial assessment of knotting in a diversity of hagfishes and Hwang et al. (2019) developed a preliminary knotting virtual simulation. Looseness may increase a skin's surface area over which dissolved organic matter may be absorbed. Glover et al. (2011) note that hagfishes are the first vertebrates to be shown to acquire nutrients directly in this fashion. Loose skin may also provide extensibility to compensate for relatively low puncture forces and stresses. Our comparison of a myxinine and an eptatretine represents a diversity of structural and behavioral characteristics in hagfishes that may be useful to compare in future studies. Myxine glutinosa tends to be behaviorally stiffer, as they do not coil when at rest (Haney et al. 2020). In contrast, E. stoutii prefers to coil its body in loops (Miyashita and Palmer 2014) and has non-muscular inclusions that take magenta stain in their skin. The nature of this histochemical difference in the skins of myxinines and eptatretines and its functional implication has not yet been investigated.

Our survey of loose skins and their putative functions seem to occur in nature primarily when freedom of movement is required (Table 1). Loose skins may also be adaptations to increase extensibility, to increase surface, or to form lubricative sheaths. There were a number of examples that would not fit into these four main categories (listed in "other" in Table 1). However, these generally maladaptive characters appear to be not operating under natural selection, and instead seem to be the result of artificial or sexual selection. With this categorization scheme, we hope to begin better understanding the functional significance of loose skins in biological examples and, in turn, perhaps identify useful design elements for human-engineered structures.

References

Adam, H. 1960. Different types of body movement in the hagfish, *Myxine glutinosa*. Nature, **188**(4750): 595–596. doi:10.1038/188595a0.

Allen, J.J., Bell, G.R.R., Kuzirian, A.M., Velankar, S.S., and Hanlon, R.T. 2014. Comparative morphology of changeable skin papillae in octopus and cuttlefish. J. Morphol. **275**(4): 371–390. doi:10.1002/jmor.20221. PMID: 24741712.

American Concrete Institute (ACI). 2006. ACI Committee 360R-06. Design of slabs-on-ground. ACI, Farmington Hills, Mich. Available from https://www.nicfi.org/files/Design%20of%20Slabs-on-Ground.pdf [accessed 1 November 2019].

American Society for Testing and Materials (ASTM). 1990. Active Standard ASTM F1306-16. Standard test method for slow rate penetration resistance of flexible barrier films and laminates. American Society for Testing and Materials, West Conshohocken, Pa. Available from https://www.astm.org/Standards/F1306.htm [accessed 25 July2018].

Barley, S.C., Mehta, R.S., Meeuwig, J.J., and Meekan, M.G. 2016. To knot or not? Novel feeding behaviours in moray eels. Mar. Biodiv. **46**(3): 703–705. doi:10.1007/s12526-015-0404-y.

Bexton, S. 2016. Hedgehogs. Ch. 12. *In* BSAVA Manual of Wildlife Casualties. 2nd ed. *Edited by* E. Mullineaux and E. Keeble. British Small Animal Veterinary Association, Gloucester, U.K. pp. 117–136.

Boggett, S., Stiles, J.L., Summers, A.P., and Fudge, D.S. 2017. Flaccid skin protects hagfishes from shark bites. J. R Soc. Interface, **14**(137): 20170765. doi:10.1098/rsif.2017.0765.

Brenner, M., and Hearing, V.J. 2008. The protective role of melanin against UV damage in human skin. Photochem. Photobiol. **84**(3): 539–549. doi:10.1111/j.1751-1097.2007.00226.x. PMID:18435612.

Caudle, H., Mehta, R., Uyeno, T.A., and Clark, A.J. 2019. Are loose skins required for moray eel knotting? Int. Comp. Biol. **59**: E286.

Clark, A.J., and Summers, A.P. 2012. Ontogenetic scaling of the morphology and biomechanics of the feeding apparatus in the Pacific hagfish, *Eptatretus stoutii*. J. Fish Biol. **80**(1): 86–99. doi:10.1111/j.1095-8649.2011.03145.x.

Clark, A.J., and Triblehorn, J.D. 2014. Mechanical properties of the cuticles of three cockroach species that differ in their wind-evoked escape behavior. PeerJ, **2**: e501. doi:10.7717/peerj.501. PMID:25101230.

Clark, A.J., and Uyeno, T.A. 2019. Feeding in jawless fishes, *In* Feeding in Vertebrates — Evolution, Morphology, Behavior, Biomechanics. *Edited by* V. Bels and I.Q. Whishaw. Springer, New York. pp. 189–230.

Clark, A.J., Crawford, C.H., King, B.D., Demas, A.M., and Uyeno, T.A. 2016. Material properties of hagfish skin, with insights into knotting behaviors. Biol. Bull. **230**(3): 243–256. doi:10.1086/BBLv230n3p243. PMID:27365419.

Clark, R.B., and Cowey, J.B. 1958. Factors controlling the change of shape of certain nemertean and turbellarian worms. J. Exp. Biol. **35**: 731–748.

Clubb, B.L., Clark, A.J., and Uyeno, T.A. 2019. Powering the hagfish "bite": The functional morphology of the retractor complex of two hagfish feeding apparatuses. J. Morphol. **280**(6): 827–840. doi:10.1002/jmor.20986. PMID: 30927384.

Collier, R. 2011. Vital or vestigial? The foreskin has its fans and foes. Can. Med. Assoc. J. **183**(17): 1963–1964. doi:10.1503/cmaj.109-4014.

Daley, M.A., and Usherwood, J.R. 2010. Two explanations for the compliant running paradox: reduced work of bouncing viscera and increased stability in uneven terrain. Biol. Lett. **6**(3): 418–421. doi:10.1098/rsbl.2010.0175. PMID:20335198.

Dalton, J.P., Skelly, P., and Halton, D.W. 2004. Role of the tegument and gut in nutrient uptake by parasitic platyhelminths. Can. J. Zool. **82**(2): 211–232. doi:10.1139/z03-213.

Danos, N., Fisch, N., and Gemballa, S. 2008. The musculotendinous system of an anguilliform swimmer: muscles, myosepta, dermis, and their interconnections in *Anguilla rostrata*. J. Morphol. **269**(1): 29–44. doi:10.1002/jmor.10570. PMID:17886889.

Davidson, J. 1998. Animal models for wound repair. Arch. Dermatol. Res. **290**(14): S1–S11. doi:10.1007/PL00007448.

de Groot, J.H., and van Leeuwen, J.L. 2004. Evidence for an elastic projection mechanism in the chameleon tongue. Proc. Biol. Sci. **271**(1540): 761–770. doi:10.1098/rspb.2003.2637. PMID:15209111.

Dickerson, A.K., Mills, Z.G., and Hu, D.L. 2012. Wet mammals shake at tuned frequencies to dry. J. R. Soc. Interface, **9**(77): 3208–3218. doi:10.1098/rsif.2012.0429. PMID:22904256.

Driessens, T., Huyghe, K., Vanhooydonck, B., and Van Damme, R. 2015. Messages conveyed by assorted facets of the dewlap, in both sexes of *Anolis sagrei*. Behav. Ecol. Sociobiol. **69**(8): 1251–1264. doi:10.1007/s00265-015-1938-5.

Domskienė, J., and Strazdienė, E. 2005. Investigation of fabric shear behavior. Fibres Text East. Eur. **13**(2): 26–30.

El-Hag, E.L., and Jayaram, S.H. 2008. Effect of biological cell size and shape on killing efficiency of pulsed electric field. ICDL 2008 IEEE International Conference on Dielectric Liquids, 30 June – 3 July. pp. 1–4, Table 2.

Falcone, I., Nagni, G., and Demarie, S. 2010. Analysis of high level swim performance in relationship with the introduction of new race swimsuits. Sport Sci. Rev. **19**(1–2): 117–186.

Fernholm, B., Norén, M., Kullander, S.O., Quattrini, A.M., Zintzen, V., Roberts, C.D., et al. 2013. Hagfish phylogeny and taxonomy, with description of the new genus *Rubicundus* (Craniata, Myxinidae). J. Zool. Syst. Evol. Res. **51**: 296–307. doi:10.1111/jzs.12035.

Forster, M.E. 1997. The blood sinus system of hagfish: its significance in a low-pressure circulation. Comp. Biochem. Physiol. **116**(3): 239–244. doi: 10.1016/S0300-9629(96)00215-0.

Forster, M.E. 1998. Cardiovascular function in hagfishes. *In* The biology of hagfishes. *Edited by* J.M. Jørgensen, R.E. Weber, and H. Malte. Chapman & Hall, London. pp. 237–258.

Freedman, C.R., and Fudge, D.S. 2017. Hagfish Houdinis: biomechanics and behavior of squeezing through small openings. J. Exp. Biol. **220**(Pt. 5): 822–827. doi:10.1242/jeb.151233. PMID:28087655.

Gerringer, M.E., Drazen, J.C., Linley, T.D., Summers, A.P., Jamieson, A.J., and Yancey, P.H. 2017. Distribution, composition and functions of gelatinous tissues in deep-sea fishes. R. Soc. Open Sci. **4**: 171063. doi:10.1098/rsos.171063.

Glover, C.N., and Bucking, C. 2015. Feeding, digestion, and nutrient absorption in hagfish. *In* Hagfish biology. *Edited by* S.L. Edwards and G.G. Goss. CRC Press, New York. pp. 299–320.

Glover, C.N., Bucking, C., and Wood, C.M. 2011. Adaptations to *in situ* feeding: novel nutrient acquisition pathways in an ancient vertebrate. Proc. R Soc. B. **278**(1721): 3096–3101. doi:10.1098/rspb.2010.2784.

Grabaum, G.D., Collins, T.H., Williams, G., Sanduja, M.L., Horowitz, C., Shvartsman, B., and Thottathil, P. 2000. 085,797. Constant velocity joint boot and method of making the same. United States Patent 6. Available from https://patents.google.com/patent/US6085797A/en.

Griffin, A.S. 2008. Quick guide: Naked mole-rat. Curr. Biol. **18**(18): R844–R845. doi:10.1016/j.cub.2008.07.054.

Guimond, R.W., and Hutchison, V.H. 1973. Aquatic respiration: an unusual strategy in the Hellbender *Cryptobranchus alleganiensis alleganiensis* (Daudin). Science, **182**(4118): 1263–1265. doi:10.1126/science.182.4118.1263. PMID: 17811319.

Haney, W.A., Clark, A.J., and Uyeno, T.A. 2020. Characterization of body knotting behavior used for escape in a diversity of hagfishes. J. Zool. **310**(4): 261–272. doi:10.1111/jzo.12752.

Harris, J.E., and Crofton, H.D. 1957. Structure and function in the nematodes: internal pressure and cuticular structure in *Ascaris*. J. Exp. Biol. **34**: 116–130.

Hebrank, M.R. 1980. Mechanical properties and locomotor functions of eel skin. Biol. Bull. **158**(1): 58–68. doi:10.2307/1540758.

Hebrank, M.R., and Hebrank, J.H. 1986. The mechanics of fish skin: Lack of an "external tendon" role in two teleosts. Biol. Bull. **171**: 236–247. doi:10.2307/1541920.

Hess, R. 2008. United States Patent US 7,360,477 B2. Rope-like structure (Kernmantle rope). Available from https://patents.google.com/patent/US7360477B2.

Hoepfner, M.T., Schultz, M.C., and Schultz, J.T. 2004. Libelle self-contained anti-G ensemble: overcoming negative transfer. J. Aviation/Aerosp. Ed. Res. **13**(2): art 6. doi:10.15394/jaaer.2004.1555.

Hwang, Y., Uyeno, T.A., and Sueda, S. 2019. Bioinspired simulation of knotting hagfish. *In* Advances in visual computing: 14th International Symposium on Visual Computing, ISVC 2019, Lake Tahoe, NV, U.S.A., 7–9 October 2019, Proceedings, Part I. *Edited by* G. Bebis, R. Boyle, B. Parvin, D. Koracin, D. Ushizima, S. Chai, et al. ISVC 2019 Lecture Notes in Computer Science Book Series, vol. 11844. Springer. pp. 75–86.

Kenaley, C.P., Sanin, A., Ackerman, J., Yoo, J., and Alberts, A. 2018. Skin stiffness in ray-finned fishes: Contrasting material properties between species and body regions. J. Morphol. **279**(10): 1419–1430. doi:10.1002/jmor.20877. PMID:30117616.

Kennedy, D.F., and Cliff, W.J. 1979. A systematic study of wound contraction in mammalian skin. Pathology, **11**(2): 207–222. doi:10.3109/00313027909061947. PMID:460946.

Kier, W.M. 1992. Hydrostatic skeletons and muscular hydrostats. *In* Biomechanics (structures and systems): a practical approach. *Edited by* A.A. Biewener. IRL Press at Oxford University Press, Oxford. pp. 205–231.

Kier, W.M. 2012. The diversity of hydrostatic skeletons. J. Exp. Biol. **215**(Pt. 8): 1247–1257. doi:10.1242/jeb.056549. PMID:22442361.

Koehl, M.A.R., Quillin, K.J., and Pell, C. 2000. Mechanical design of fiber-wound hydraulic skeletons: the stiffening and straightening of embryonic notochords. Am. Zool. **40**(1): 28–41.

Krogh, A. 1929. The Progress of Physiology. Am. J. Physiol. **90**(2): 243–251. doi:10.1152/ajplegacy.1929.90.2.243.

Lillywhite, H.B. 1989. Unusual shedding behaviors in an aquatic snake, *Acrochordus granulatus*. Copeia. **1989**(3): 768–770. doi:10.2307/1445513.

Lillywhite, H.B., and Stein, B.R. 1987. Surface sculpturing and water retention of elephant skin. J. Zool. (Lond.), **211**: 727–734.

Lim, J., Fudge, D.S., Levy, N., and Gosline, J.M. 2006. Hagfish slime ecomechanics: testing the gill-clogging hypothesis. J. Exp. Biol. **209**(Pt. 4): 702–710. doi:10.1242/jeb.02067. PMID:16449564.

Long, J.H., Jr., Hale, M.E., McHenry, M.J., and Westneat, M.W. 1996. Functions of fish skin: flexural stiffness and steady swimming of longnose gar, *Lepisosteus osseus*. J. Exp. Biol. **199**(Pt. 10): 2139–2151. PMID:9320050.

Long, J.H., Jr., Adcock, B., and Root, R.G. 2002a. Force transmission via axial tendons in undulating fish: a dynamic analysis. Comp. Biochem. Physiol. A, **133**(4): 911–929. doi:10.1016/S1095-6433(02)00211-8.

Long, J.H, Jr., Koob-Emunds, M., Sinwell, B., and Koob, T.J. 2002b. The notochord of hagfish *Myxine glutinosa*: visco-elastic properties and mechanical functions during steady swimming. J. Exp. Biol. **205**(Pt. 24): 3819–3383. PMID:12432006.

Martini, F.H. 1998. The ecology of hagfishes. *In* The biology of hagfishes. *Edited by* J.M. Jørgensen, R.E. Weber, and H. Malte. Chapman & Hall, London. pp. 57–77.

McDonald, D.G., Cavdek, V., Calvert, L., and Milligan, C. 1991. Acid-base regulation in the Atlantic hagfish *Myxine glutinosa*. J. Exp. Biol. **161**: 201–215.

Miller, J.A., and Byrne, M. 2000. Ceratal autotomy and regeneration in the aeolid nudibranch *Phidiana crassicornis* and the role of predators. Invert. Biol. **119**(2): 167–176. doi:10.1111/j.1744-7410.2000.tb00005.x.

Miyashita, T., and Palmer, A.R. 2014. Handed behavior in hagfish—an ancient vertebrate lineage—and a survey of lateralized behaviors in other invertebrate chordates and elongate vertebrates. Biol. Bull. **226**(2): 111–120. doi:10.1086/BBLv226n2p111.

Miyashita, T., Coates, M.I., Farrar, R., Larson, P., Manning, P.L., Wogelius, R.A., et al. 2019. Hagfish from the Cretaceous Tethys Sea and a reconciliation of the morphological–molecular conflict in early vertebrate phylogeny. Proc. Natl. Acad. Sci. U.S.A. **116**(6): 2146–2151. doi:10.1073/pnas.1814794116.

Moghani, T., Butler, J.P., Li-Wen Lin, J., and Loring, S.H. 2007. Finite element simulation of elastohydrodynamic lubrication of soft biological tissues. Comput. Struct. **85**(11–14): 1114–1120. doi:10.1016/j.compstruc.2006.08.026. PMID:18037975.

Moore, C.R., and Quick, W.J. 1924. The scrotum as a temperature regulator for the testes. Am. J. Physiol. **68**(1): 70–79. doi:10.1152/ajplegacy.1924.68.1.70.

Muller, G.H. 1990. Skin diseases of the Chinese Shar-Pei. Vet. Clin. North Am. Small Anim. Pract. **20**(6): 1655–1670. doi:10.1016/s0195-5616(90)50166-7. PMID:2251744.

Müller, U.K., and van Leeuwen, J.L. 2006. Undulatory fish swimming: from muscles to flow. Fish Fish. **7**: 84–103. doi:10.1111/j.1467-2979.2006.00210.x.

Naldaiz-Gastesi, N., Bahri, O.A., López de Munain, A., McCullagh, K.J.A., and Izeta, A. 2018. The *panniculus carnosus* muscle: an evolutionary enigma at the intersection of distinct research fields. J. Anat. **233**(3): 275–288. doi:10.1111/joa.12840.

Naresh, M.D., Arumugam, V., and Sanjeevi, R. 1997. Mechanical behaviour of shark skin. J. Biosci. **22**(4): 431–437. doi:10.1007/BF02703189.

Nothofer, K., and Lausch, P. 2009. Patent No.: US 7,522,795 B2. Loose tube optical waveguide fiber cable. Available from https://patents.google.com/patent/US7522795B2/en.

Pieranski, P., Kasas, S., Dietler, G., Dubochet, J., and Stasiak, A. 2001. Localization of breakage points in knotted strings. New J. Phys. **3**: 10.1–10.13. doi:10.1088/1367-2630/3/1/310.

Potts, W.T.W., Foster, M.A., Rudy, P.P., and Howells, G.P. 1967. Sodium and water balance in the cichlid teleost, *Tilapia mossambica*. J. Exp. Biol. **47**(3): 461–470. PMID:5592412.

Rugh, D.J., and Shelden, K.E.W. 2009. Bowhead whale: *Balaena mysticetus*. *In* Encyclopedia of Marine Mammals. 2nd ed. *Edited by* W.F. Perrin, B. Würsig, and J.G.M. Thewissen. Elsevier/Academic Press, Boston. pp. 131–133.

Ryg, M., Lydersen, C., Knutsen, L.Ø., Bjørge, A., Smith, T.G., and Øritsland, N.A. 1993. Scaling of insulation in seals and whales. J. Zool. (Lond.). **230**(2): 193–206. doi:10.1111/j.1469-7998.1993.tb02682.x.

Satchell, G.H. 1984. On the caudal heart of *Myxine* (Myxinoidea: Cyclostomata). Acta Zool. (Stockh.), **65**(3): 125–133. doi:10.1111/j.1463-6395.1984.tb00818.x.

Shadwick, R.E., Russell, A.P., and Lauff, R.F. 1992. The structure and mechanical design of rhinoceros dermal armour. Philos. Trans. R. Soc. Lond. B Biol. Sci. **337**(1282): 419–428. doi:10.1098/rstb.1992.0118. PMID:1359589.

Smart, C. 1885. The works of Horace. First book of the Epistles of Horace; Epistle X to Aristius Fuscus. *Edited by* T.A. Buckley. American Book Co., New York. pp. 1–249.

Smith, J.P.S., Litvaitis, M.K., Gobert, S., Uyeno, T., and Artois, T. 2015. Evolution and functional morphology of the proboscis in Kalyptorhynchia (Platyhelminthes). Integr. Comp. Biol. **55**(2): 205–216. doi:10.1093/icb/icv056. PMID:26002347.

Strahan, R. 1963. The behaviour of myxinoids. Acta Zool.3 **44**(1-2): 73–102. doi:10.1111/j.1463-6395.1963.tb00402.x.

Stricker, S.A. 1985. The ultrastructure and formation of the calcareous ossicles in the body wall of the sea cucumber *Leptosynapta clarki* (Echinodermata, Holothuroida). Zoomorphology, **105**(4): 209–222. doi:10.1007/BF00311965.

Sullivan, J.S. 1982. United States Patent US4356569A Armored skin diving suit. Available from https://patents.google.com/patent/US4356569A/en.

Summers, A.P., and Long, J.H., Jr. 2005. Skin and bones, sinew and gristle: the mechanical behavior of fish skeletal tissues. Fish Physiol. **23**: 141–177. doi:10.1016/S1546-5098(05)23005-4.

Thapar, V. 2004. Tiger: the ultimate guide. CDS Books, New York.

Trinidad Morales, A., Tamayo Fajardo, J.A., and González-García, H. 2019. High-speed swimsuits and their historical development in competitive swimming. Front. Psychol. **10**: 2639. doi:10.3389/fpsyg.2019.02639. PMID:31920770.

Turner, A. 1997. The big cats and their fossil relatives: an illustrated guide to their evolution and natural history. Columbia University Press, New York.

Uyeno, T.A., and Clark, A.J. 2016. Why do some things have loose skins? Poster P3.119. at the Society for Integrative and Comparative Biology Annual General Meeting 2016, Portland, Oregon, 3–7 January 2016.

Verberkt, R.M., Janssen, M., and Wesseling, J. 2013. A boy with tight skin: borrelia-associated early-onset morphea. Clin. Exp. Rheumatol. **31**: 121–122. PMID:24093617.

Vincent, J.F.V., and Wegst, U.G. 2004. Design and mechanical properties of insect cuticle. Arthropod Struct. Dev. **33**(3): 187–199. doi:10.1016/j.asd.2004.05.006. PMID:18089034.

Viborg, A.L., and Hillyard, S.D. 2005. Cutaneous blood flow and water absorption by dehydrated toads. Physiol. Biochem. Zool. **78**(3): 394–404. doi:10.1086/430225. PMID:15887086.

Vogel, S. 2013. Comparative biomechanics: life's physical world. Princeton University Press, Princeton, N.J.

Voute, C.L. 1963. An electron microscopic study of the skin of the frog (*Rana pipiens*). Ultrastruct. Res. **9**(5–6): 497–510. doi:10.1016/S0022-5320(63)80081-7.

Wainwright, S.A., Vosburgh, F., and Hebrank, J.H. 1978. Shark skin: function in locomotion. Science, **202**(4369): 747–749. doi:10.1126/science.202.4369.747. PMID:17807247.

Wright, G.M. 1984. Structure of the conus arteriosus and ventral aorta in the sea lamprey, *Petromyzon marinus*, and the Atlantic hagfish, *Myxine glutinosa*: microfibrils, a major component. Can. J. Zool. **62**(12): 2445–2456. doi:10.1139/z84-361.

Yang, W., Chen, I.H., McKittrick, J., and Meyers, M.A. 2012. Flexible dermal armor in nature. JOM, **64**(4): 475–485. doi:10.1007/s11837-012-0301-9.

Zheng, Y. 2019. The co-occurrence of loose skin and underwater calling in frogs—further evidence from *Amolops ricketti* and its implications. J. Zool. **309**(4): 280–286. doi:10.1111/jzo.12722.

Zintzen, V., Roberts, C.D., Anderson, M.J., Stweart, A.J., Struthers, C.D., and Harvey, E.S. 2011. Hagfish predatory behaviour and slime defence mechanism. Sci. Rep. **1**: 131. doi:10.1038/srep00131.